Computational Modeling of Nanosecond Time-Scale Charge Carrier Dynamics in Organic Semiconductors

Journal:	*2014 MRS Fall Meeting*
Manuscript ID:	2043646.R1
Manuscript Type:	Symposium U
Date Submitted by the Author:	n/a
Complete List of Authors:	Johnson, Brian; Oregon State University, Paudel, Keshab; Oregon State University, Ostroverkhova, Oksana; Oregon State University,
Keywords:	photoconductivity, organic, electronic material

Computational modeling of nanosecond time-scale charge carrier dynamics in organic semiconductors

Brian Johnson[1], Keshab Paudel[1], Oksana Ostroverkhova[1]

[1]Oregon State University, Corvallis, OR, United States

ABSTRACT

We present a study of photoinduced charge carrier dynamics in single crystals and polycrystalline thin films of a functionalized fluorinated anthradithiophene (ADT) derivative, ADT-TES-F, combining measurements of time-resolved photocurrent with computational modeling. Simulations revealed two competing charge generation pathways: ultrafast charge separation and nanosecond (ns) time-scale exciton dissociation. Single crystals exhibited significantly enhanced fast charge photogeneration and charge carrier mobilities, as well as lower charge trap densities and free hole-trapped electron recombination, as compared to thin films. At sub-ns time scales after photoexcitation, the light intensity dependence of the photocurrents obtained in single crystals was determined by the carrier density-dependent recombination. At longer time scales, and at lower intensities, taking into account carrier concentration-dependent mobility improved agreement between numerically simulated and experimentally measured photocurrent data.

INTRODUCTION

Organic semiconductors are of interest for (opto)electronic applications due to their ease of fabrication, low cost, and tunable properties. A considerable research effort has been applied to characterizing charge photogeneration and transport, as well as structure-property relationships, in small-molecule and polymeric materials.[1,2] One promising class of organic materials is solution-processable small-molecule organic semiconductors with high charge carrier mobilities and strong photoresponse. Examples of such materials are functionalized anthradithiophene (ADT) derivatives which display fast photoresponse, thin-film transistor (TFT) charge carrier (hole) mobilities of ~1.5 cm^2/Vs in spin-cast films, and high photoconductive gains under continuous wave excitation.[3,4] However, understanding of mechanisms of enhanced charge photogeneration and charge transport in these materials is lacking and is necessary for guiding design of improved materials. To address these issues, we developed in our previous work a numerical model which allowed us to analyze photocurrent dynamics in polycrystalline thin films of functionalized ADT derivatives[5–7] and bulk heterojunctions with the ADT donor. In particular, we quantified the contributions of various charge generation pathways and of charge carrier transport, trapping, and recombination properties to experimentally measured time-resolved photocurrents (TPCs). Here, we extend this work to single crystal devices, which are good model systems for studies of *intrinsic* properties of the material, and compare various parameters pertaining to photoinduced charge carrier dynamics in single crystals and thin films of a fluorinated ADT derivative functionalized with triethylsilylethynyl (TES) side groups, ADT-TES-F (Fig. 1b, inset).

One of the tests of robustness for a model describing photocurrent dynamics is the model's ability to predict dependence of the charge carrier dynamics on various external parameters such as electric field, light intensity, and temperature. Previously, we modeled the electric field

dependence of the TPC dynamics which result from that of the charge photogeneration efficiency and charge carrier mobility.[5] In this paper, we focus on the origin of *light intensity*-dependent TPC and, in particular, explore contributions of charge carrier density-dependent recombination (such as bimolecular recombination) and mobility to the TPC amplitude and dynamics. The dependence of mobility on charge carrier concentration (defined as the ratio of free charge carrier and total hopping site densities)[8] has primarily been explored in field-effect transistors, where the carrier concentration can be controlled by varying the gate voltage.[9] However, the field-effect mobility is strongly affected by charge trapping and metal-organic interface effects, which obscure the direct effect of carrier concentration on charge transport. Carrier concentration dependence in the low-mobility ($\mu<10^{-3}$ $cm^2/(Vs)$) polymers with hopping charge transport has been extensively studied theoretically.[8] A review of several numerical models found that the carrier density dependence of mobility could be parametrized by a simple exponential.[8] These models utilize a Miller-Abrahams's hopping rate and a Gaussian density of states (DOS), the applicability of which to materials with higher mobilities ($\mu > \sim 1$ cm^2/Vs) such as organic single crystals, is still under debate[9–13]and is explored here.

THEORY

A detailed overview of the model used, which describes TPC dynamics in both pristine materials and their donor-acceptor (D/A) blends, can be found elsewhere.[5–7] Briefly, we solve a system of space-averaged coupled differential equations to determine the time evolution of free and trapped charge carrier densities and of exciton density under pulsed light excitation. The model incorporates multiple charge generation paths, electron and hole trapping, hole detrapping, trap assisted recombination, and bimolecular recombination. In pristine materials, the two charge generation paths considered are ultrafast formation of spatially separated carriers (SSC) with efficiency ξ_{SSC} and formation (with efficiency ξ_{FE}) and dissociation of Frenkel excitons (FEs) during their lifetimes τ (typically >10 ns) with efficiency η; these were previously quantified in pristine films of ADT-TES-F (inset of Fig.1(b)) and its D/A blends.[5–7] Here we explore (i) the differences between time-resolved charge carrier dynamics in film and single crystal and (ii) the light intensity-dependent photocurrent dynamics in single crystals. For (ii), we tested two hypotheses: charge carrier density-dependent recombination and charge carrier density-dependent mobility, respectively, as the dominant factor. For that, we have modified the temperature (T)- and electric field (E)-dependent Poole-Frenkel charge carrier mobility[5–7] $\mu_{p(n)0}\left(T,E\right)$ to incorporate a carrier density dependence as follows:

$$\mu_{p(n)} = \mu_{p(n)0}\left(T,E\right) * f_m\left(p(n)_f, T\right) \quad (1)$$

$$f_1\left(p(n)_f\right) = 1 \quad (2)$$

$$f_2\left(p(n)_f\right) = exp\left(u_{p(n)}\left(2p(n)_f / N_t\right)^{v_{p(n)}}\right) \quad (3)$$

where $p(n)_f$ is the free hole (electron) density and $f_m\left(p(n)_f, T\right)$ is a carrier density dependence function (Eqs.(2) and (3)). The function f_1 (Eq. (2)) assumes no carrier density dependence of mobility, previously predicted for the case of carrier concentrations of 10^{-4}-10^{-6} carriers/site, similar to ours.[14] Therefore, the light intensity-dependent TPC dynamics simulated using f_1 would be due to carrier density-dependent recombination only. The function f_2 (Eq.(3)) is a parametrization of numerical hopping conduction results derived by Coehoorn et al.,[8] which

assumes a Gaussian DOS with width $\sigma_{p(n)}$ for hole(electron) conduction. N_t is the number of possible hopping sites (taken to be 10^{20} cm^{-3}), $u_{p(n)} = (1/2)(\hat{s}_{p(n)}^2 - \hat{s}_{p(n)})$, $v_{p(n)} = (2/\hat{s}_{p(n)}^2)(\ln(\hat{s}_{p(n)}^2 - \hat{s}_{p(n)}) - \ln(\ln(4)))$, $\hat{s}_{p(n)} = \sigma_{p(n)}/k_BT$. In this approach, charge carrier mobility is an increasing function of carrier concentration, which in our experiments is light intensity-dependent. Therefore, in this case the TPC incorporates intensity-dependent contributions of mobility and of various mobility-dependent rates.[5] In our model, the mobility-dependent rates are bimolecular recombination and FE dissociation; both rates have a linear dependence on mobility.[5]

Using carrier density-dependent mobility with function f_2 also requires a change in how initial conditions are calculated. In particular, we must now numerically solve the following equations to determine initial conditions (i.e. in the dark, before photoexcitation) for holes and electrons as a system:[5]

$$n_f^0 e^{\frac{\varphi_B^n}{k_BT}} \left(\mu_{n0} f_m\left(n_f^0, T\right) e^{\frac{-\varphi_B^n}{k_BT}} + \mu_{p0} f_m\left(p_f^0, T\right) e^{\frac{-\varphi_B^p}{k_BT}} \right) = \frac{J_{Dark}}{eE} \tag{4}$$

$$p_f^0 e^{\frac{\varphi_B^p}{k_BT}} \left(\mu_{n0} f_m\left(n_f^0, T\right) e^{\frac{-\varphi_B^n}{k_BT}} + \mu_{p0} f_m\left(p_f^0, T\right) e^{\frac{-\varphi_B^p}{k_BT}} \right) = \frac{J_{Dark}}{eE} \tag{5}$$

where $p(n)_f^0$ is the initial hole (electron) density, J_{Dark} is the measured dark current density at the applied electric field E, k_B is Boltzmann's constant, and $\phi_B^{p(n)}$ is the injection barrier for holes (electrons), taken to be 0.25 (2.05) eV.

RESULTS AND DISCUSSION

Polycrystalline films of ADT-TES-F were spin cast from chlorobenzene solution onto pentafluorobenzenethiol (PFBT)-treated interdigitated Au electrodes with a 25 μm gap deposited on glass substrates. Similar substrates were used for single crystal growth, for which a 30 mM chlorobenzene solution of ADT-TES-F was deposited on the substrate which was then placed in the refrigerator. Such procedure yielded >100 μm size crystals, which were then separated and characterized using polarization microscopy. The samples were excited with a 470 ps 532 nm laser, and the TPCs were measured using a 50 GHz digital sampling oscilloscope, as described in detail in our previous publications.[5,7] The time resolution was about 0.5 ns, limited by the laser pulse width. The incident pulse fluence was varied using a Thorlabs neutral density filter wheel in the 2 – 39 μJ/cm^2 range. The experimental data were then fit with numerically simulated photocurrents, and various parameters of the model were determined as detailed elsewhere.[5]

Single crystal versus thin film

The examples of simulated photocurrents obtained for the thin film and single crystal devices using f_1 and the parameter values reported in Table I (col 1 & 3) are presented in Fig. 1. Table I also includes results from a fit of single crystal TPC at 20 kV/cm and 5 μJ/cm^2. The single crystal devices exhibited considerably higher peak photocurrent densities and slower initial decay dynamics as compared to those in thin film samples (Fig.1). The ultrafast SSC charge generation pathway (characterized by ξ_{SSC}, Table I) was significantly more efficient in single

crystals than in films, consistent with previous work showing a strong dependence of SSC efficiency on film crystallinity.[7] In contrast, the FE dissociation-based contribution to charge generation (ξ_{FE}*η) was considerably reduced in the single crystal, which could be related to a considerably higher FE recombination rate k_R as compared to that in films (Table I). The rate of the initial photocurrent decay depends on charge carrier recombination and trapping properties; for example, faster initial decay in ADT-TES-F/PCBM blends as compared to pristine ADT-TES-F films has previously[7] been attributed to bimolecular recombination. A considerably slower initial decay rate in single crystal devices as compared to thin films (Fig. 1) is a combination of reduced trap densities (N_p and N_n), shallower traps (Δ), and reduced free hole-trapped electron recombination ($B_{p_f n_t}$) in the single crystal (Table I).

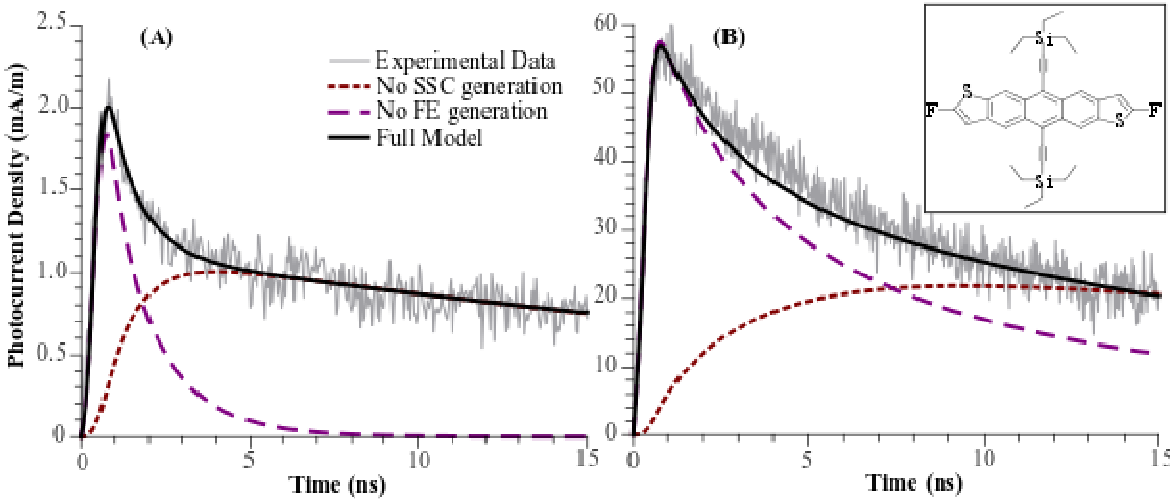

Figure 1. Experimental (grey) and simulated (black) TPC densities for (A) a thin film at 50 kV/cm and 2 $\mu J/cm^2$ and (B) a single crystal at 20 kV/cm and 24 $\mu J/cm^2$. Other lines show simulations run with $\xi_{SSC} = 0$ (dotted line) and $\xi_{FE} = 0$ (dashed line). Inset shows the molecular structure of ADT-TES-F.

Table I. Selected parameter values extracted from fits of experimental data to the numerical model[5] using f_1. Column 3 used a similar procedure to our previous voltage dependent fits.[5]

Sample:	1. Thin Film 2 $\mu J/cm^2$	2. Single Crystal 5 $\mu J/cm^2$	3. Single Crystal 5-39 $\mu J/cm^2$
$\mu_{n0}(T,E)$ (cm^2/Vs)	0.2	0.7	0.7
$\mu_{p0}(T,E)$ (cm^2/Vs)	0.9	2.0	2.1
ξ_{SSC}	0.04	0.22	0.24
ξ_{FE}*η	0.33	0.05	0.05
$k_{Diss,FE}$ (s^{-1})	2.6×10^7	1.7×10^7	1.7×10^7
k_R (s^{-1})	1.0×10^7	7.6×10^7	7.6×10^7
N_n (cm^{-3})	3.0×10^{19}	3.2×10^{18}	3.5×10^{18}
N_p (cm^{-3})	4.4×10^{18}	2.7×10^{18}	3.7×10^{18}
$B_{n_f p_t}$ (cm^3/s)	1.9×10^{-3}	4.8×10^{-3}	4.0×10^{-3}
$B_{p_f n_t}$ (cm^3/s)	2.1×10^{-6}	1.6×10^{-7}	9.4×10^{-8}
Δ (meV)	31	20	15

Light intensity dependence of photocurrent dynamics

Comparisons between TPC fits using f_1 and f_2 functions (Eqs. (2) & (3)) at multiple incident intensities in the single crystal sample are shown in Figure 2. Although both f_1 and f_2 approaches could reproduce the data reasonably well at particular light intensities (e.g. Fig. 2A), neither f_1 nor f_2 fully captured the TPC dynamics over the entire light intensity range studied (Fig. 2B-D), which corresponded to carrier concentrations of 10^{-5}-10^{-4} carriers/site. Figures 2C and 2D show TPCs integrated over a 20 ns time period and TPC peak amplitudes, respectively, obtained from experimental data (circles) and numerically simulated TPCs using f_1 (squares) and f_2 (diamonds). The f_1 approach slightly overestimated the TPC amplitude throughout the entire intensity range and overestimated the extracted charge at low intensities. The f_2 approach predicted a stronger intensity dependence of the TPC amplitude than the one observed experimentally, but matched the change in the extracted charge with intensity better than f_1 throughout the entire intensity range. This indicates that light intensity dependence of the TPC dynamics at sub-ns time scales (reflected in that of the TPC amplitude) is mostly determined by charge carrier density-dependent recombination (bimolecular and/or trap-assisted), in which mobility does not depend on carrier concentration. However, at longer time scales (reflected in the integrated TPC), and at low intensities (<10 μJ/cm^2), additional intensity-dependent contributions may become

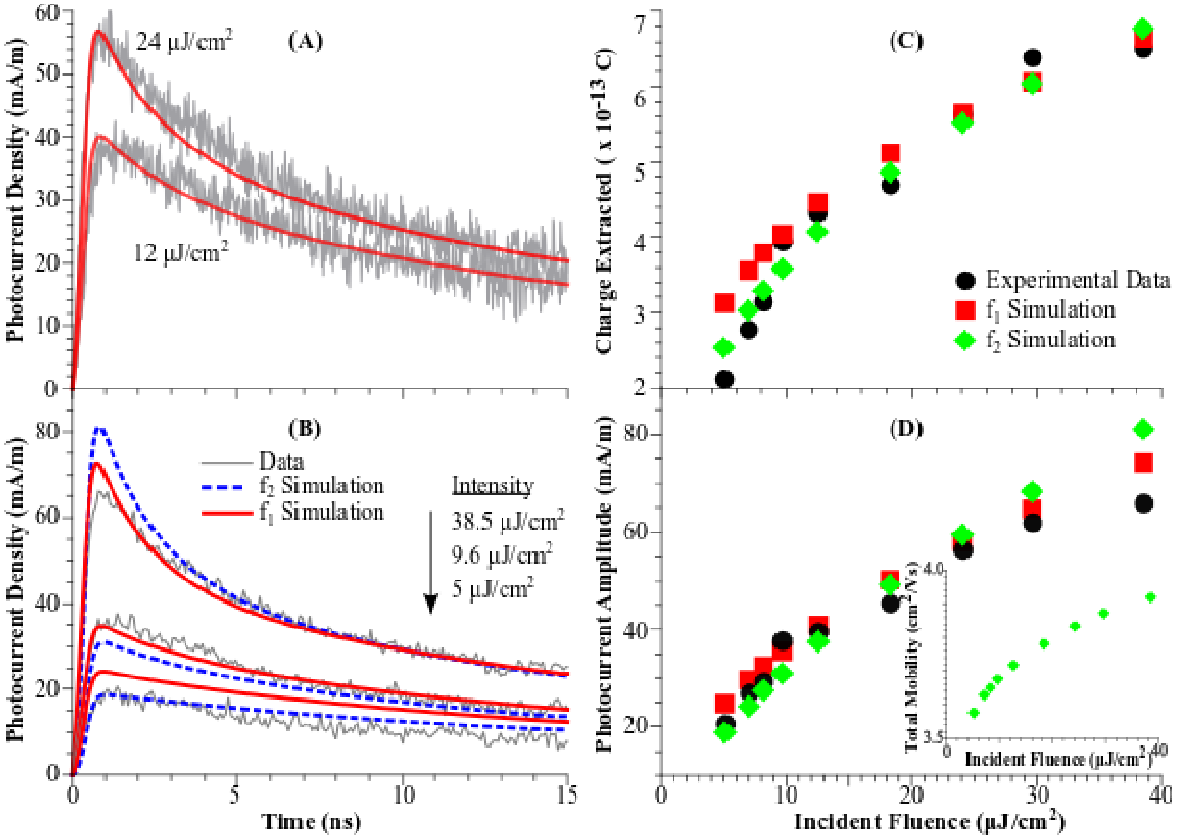

Figure 2. (A) TPC data along with simulations using f_1 for two light intensities. (B) TPC data and simulations using f_1 and f_2 for multiple intensities. (C) Integrated TPC photocurrent values and (D) TPC amplitude for experiment and simulations using f_1 and f_2. Inset: Sum of mobilities ($\mu_n + \mu_p$) calculated using f_2 for multiple intensities.

important. This includes carrier density-dependent charge carrier mobility, for which the simulations using the f_2 approach predicted about a ~10% increase in an overall mobility in the range of light intensities used in our experiments (Fig. 2D, inset).[8]

CONCLUSIONS

We applied a numerical model to an analysis of experimentally measured time-resolved photocurrent dynamics[5,7] in ADT-TES-F single crystal and thin film devices. Contributions of several charge photogeneration pathways to the photocurrent were quantified, and parameters describing charge transport, trapping, and recombination properties were determined. In single crystals, we observed large enhancements in the ultrafast charge carrier separation efficiency and in charge carrier mobilities, as well as reduction in charge trap densities and in free hole-trapped electron recombination, as compared to thin films. In single crystals at sub-ns time scales after photoexcitation, the light intensity dependence of the photocurrent is largely determined by the carrier density-dependent recombination. At longer time scales, and at lower intensities, taking into account carrier concentration-dependent mobility improves agreement between numerically simulated and experimentally measured photocurrent data.

ACKNOWLEDGMENTS

We thank Prof. J.E. Anthony for ADT-TES-F and Prof. O. D. Jurchescu for single crystal samples for our initial studies and for helpful tips on the single crystal growth. This work was supported by the NSF grant DMR-1207309.

REFERENCES

[1] T. Clarke and J. Durrant, Chem. Rev. **110**, 6736 (2010).
[2] B. Walker, C. Kim, and T.-Q. Nguyen, Chem. Mater. **23**, 470 (2011).
[3] R.J. Kline, S.D. Hudson, X. Zhang, D.J. Gundlach, A.J. Moad, O.D. Jurchescu, T.N. Jackson, S. Subramanian, J.E. Anthony, M.F. Toney, and L.J. Richter, Chem. Mater. **23**, 1194 (2011).
[4] A.D. Platt, J. Day, S. Subramanian, J.E. Anthony, and O. Ostroverkhova, J. Phys. Chem. C **113**, 14006 (2009).
[5] B. Johnson, M.J. Kendrick, and O. Ostroverkhova, J. Appl. Phys. **114**, 094508 (2013).
[6] B. Johnson, K. Paudel, M.J. Kendrick, and O. Ostroverkhova, Proc. SPIE **8830**, 88301S (2013).
[7] K. Paudel, B. Johnson, M. Thieme, M.M. Haley, M.M. Payne, J.E. Anthony, and O. Ostroverkhova, Appl. Phys. Lett. **105**, 043301 (2014).
[8] R. Coehoorn, W. Pasveer, P. Bobbert, and M. Michels, Phys. Rev. B **72**, 155206 (2005).
[9] H. Sirringhaus, T. Sakanoue, and J.-F. Chang, Phys. Stat. Sol. B **249**, 1655 (2012).
[10] H. a v Laarhoven, C.F.J. Flipse, M. Koeberg, M. Bonn, E. Hendry, G. Orlandi, O.D. Jurchescu, T.T.M. Palstra, and A. Troisi, J. Chem. Phys. **129**, 044704 (2008).
[11] Y.C. Cheng, R.J. Silbey, D. A. da Silva Filho, J.P. Calbert, J. Cornil, and J.L. Brédas, J. Chem. Phys. **118**, 3764 (2003).
[12] J. Cottaar, L. Koster, R. Coehoorn, and P. Bobbert, Phys. Rev. Lett. **107**, 136601 (2011).
[13] A. Troisi, J. Chem. Phys. **134**, 034702 (2011).
[14] M.E. Gershenson, V. Podzorov, and A.F. Morpurgo, Rev. Mod. Phys. **78**, 973 (2006).